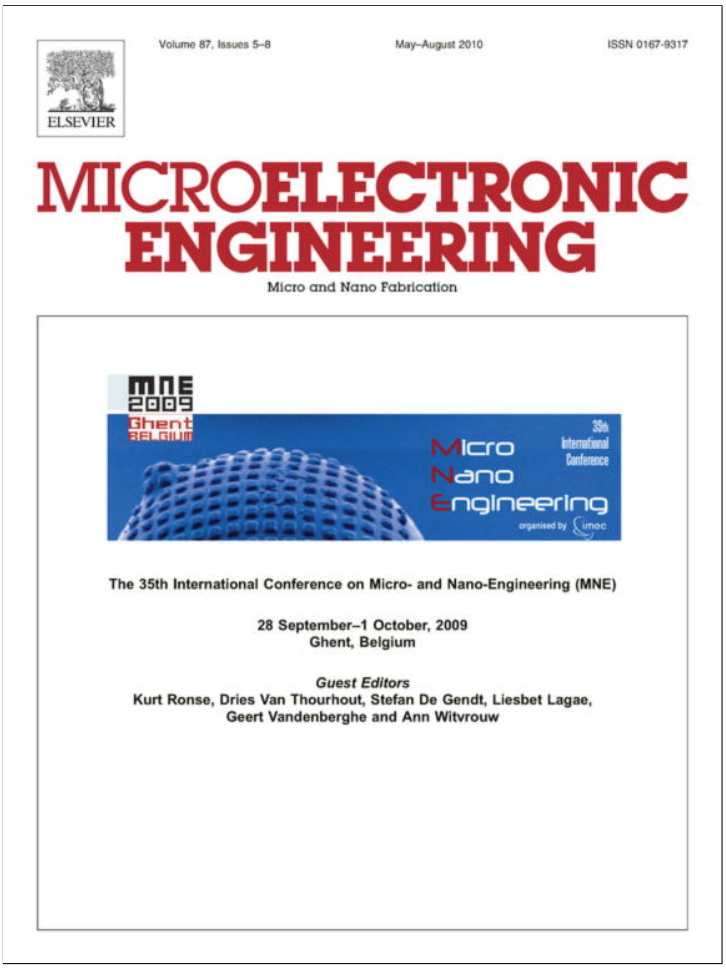

Microelectronic Engineering 87 (2010) 1455–1457

Contents lists available at ScienceDirect

Microelectronic Engineering

journal homepage: www.elsevier.com/locate/mee

Simulation of the nanostructuring of surfaces under ion-beam bombardment

Florin Fulga, Dan V. Nicolau *

Department of Electrical Engineering and Electronics, University of Liverpool, L69 3GJ, United Kingdom

ARTICLE INFO

Article history:
Received 14 September 2009
Received in revised form 18 November 2009
Accepted 20 November 2009
Available online 3 December 2009

Keywords:
Nanolithography
Ion-beam
Self-assembly

ABSTRACT

As top-down nanolithography is inexorably approaching its ultimate limits, the techniques based on bottom-up self-assembly become increasingly attractive. Among these, the ion-beam-induced self-assembly of thin films occupies a special place, as they combine both the top-down, focused micro-fabrication with the bottom-up self-assembly nano-processes. Because the ion-beam-induced self-assembly processes are not well understood, here we report on the design-orientated modelling and simulation of quasi-organised metallic nanostructures. It has been found that, because of the near-critical state of the ion-beam-induced self-assembly, the interplay between the angle of ion bombardment, ion flux and substrate temperature leads to nanotopographies that are either quasi-structured or random. Furthermore, minor variations in the angle of bombardment leads to a large variation of the parameters of the nano-organisation, i.e., the type of the ripples – lateral or transversal, and ripple wavelengths. The simulation results were benchmarked against comprehensive experimental results reported in the literature. This study demonstrates that simulation can be used in a feed-forward, design-orientated manner when attempting the fabrication of self-assembled nanostructures with micron-level ion-beam techniques.

1. Introduction

As top-down nanolithography is inexorably approaching its ultimate limits, various techniques able to provide quasi-ordered nanostructures by self-organisation have been reported [1]. Among these, the low energy ion-beam-induced self-assembly occupy a special place as it combines both fabrication strategies, i.e., top-down, radiation-based technique, with regions of interest spanning from tens of nanometres to microns, with the bottom-up self-assembly processes of liquefied metals operating in the region of few to tens of nanometres. Moreover, this technique is capable of producing nanostructures on diverse substrates such as Si, GaSb, InP or metallic thin films. Despite an almost a decade of research of these processes, it appears that the ion-beam self-assembly processes are not fully understood, let alone being predicted, because of the extreme sensitivity of the self-assembly process conditions. This is unfortunate, as the fabrication of quasi-organised nanostructures, especially on larger areas would find extensive applications in many areas, especially biomedical-orientated, e.g., surfaces that mimic the molecular surface of biomolecules.

Here, we report on the process-design-orientated simulation of the self-assembly processes induced by ion-beam irradiation and characterisation/classification of the surface morphology using the methods of image processing and pattern recognition. In order to compare the morphology of different materials obtained by ion-beam irradiation, several techniques have been employed: time dependent Fourier transform, time dependent rms fluctuations in height, and moment invariants. The overall goal of such an analysis is to reach conclusions regarding the classification of nanostructured surfaces, and, thus to be able to design process conditions tailored for a specific application.

2. Modelling and simulation methodology

The temporal evolution of the experimentally observed pattern formation can be described by a partial differential equation based on the Sigmund's sputtering theory [2]. The amplification of a surface modulation is the result of the difference between the local sputtering yields, higher at the bottom of the valleys, lower at top of the hills. A linear differential equation describing the temporal development of the surface profile $h(x, y, t)$, introduced by Bradley and Harper [3], describes certain characteristics of the topography, but being a linear equation, there is no term to limit the exponential growth of ripples amplitude. An extension of this model is based on the nonlinear anisotropic stochastic equation, known as Kuramoto–Sivashinsky (KS) equation [4].

$$\frac{\partial h}{\partial t} = \upsilon_x \frac{\partial^2 h}{\partial x^2} + \upsilon_y \frac{\partial^2 h}{\partial y^2} - K_x \frac{\partial^4 h}{\partial x^4} - K_{xy} \frac{\partial^4 h}{\partial x^2 y^2} - K_y \frac{\partial^4 h}{\partial y^4} + \frac{\lambda_x}{2}\left(\frac{\partial h}{\partial x}\right)^2 + \frac{\lambda_y}{2}\left(\frac{\partial h}{\partial y}\right)^2 + \eta(x, y, t)$$

* Corresponding author. Tel.: +44 151 794 4537; fax: +44 151 794 4540.
E-mail address: dnicolau@liverpool.ac.uk (D.V. Nicolau).

0167-9317/$ - see front matter Crown Copyright © 2009 Published by Elsevier B.V. All rights reserved.
doi:10.1016/j.mee.2009.11.110

Here, $h(x, y, t)$ is the height; $\upsilon_{x,y}$ are effective surface tension generated by the erosion process; $K_{x,xy,y}$ are surface diffusion constants; $\lambda_{x,y}$ are parameter describing the tilt-dependent erosion rate; and $\eta(x, y, t)$ is uncorrelated white noise with zero mean, mimicking the stochastic nature of the ion arrival to the surface.

The coefficients depend in a complex manner on the technological and microscopic parameters. The technological parameters, i.e., J is the ion flux, ε is the total energy carried by the ion, p is the material constant, θ is the angle of incidence, are all parameters with well-determined values. The microscopic parameters, i.e., a is the mean energy depth, σ and μ are the width of the distribution in directions parallel and perpendicular to the incoming beam, are values that are either measured experimentally or estimated by simulation, with differences between reported values for these parameters reaching 7-fold [5]. The coefficients appearing in KS equation are calculated here using the relations given in Makeev et al. [6].

As the temperature dependence of the physical processes is highly critical for this system [3], we coupled the above-mentioned formalism with the 3D heat conduction equation to describe the local temperature evolution of the surface.

$$\rho \cdot c(T)\frac{\partial T}{\partial t} = -\nabla(k(T)\cdot\nabla T) + f(t)\cdot P(e,x,y)$$

Here, ρ is the target density, $c(T)$ is the heat capacity, $k(T)$ is the thermal conduction coefficient, $f(t)$ is the time form of the ion-beam (for pulsed ion-beam), $P(e, x, y)$ is the energy release function, e is the ion energy, T is the temperature, and t is the time.

The actual local temperature in the sample dictates the values of various model parameters. For the variation with temperature, two cases were considered: (i) the ion-beam exposure at constant temperature, with model parameters estimated for this temperature; and (ii) the ion-beam exposure with varying temperature for long sputtering times, when the equation of heat transfer was solved and the local temperature was calculated rather than imposed.

In order to compare easily with the experimental results [5,7–9], the KS equation was scaled and used in dimensionless form.

The numerical integration was performed with a commercial finite element package from COMSOL Multiphysics.

3. Results and discussion

The aim of the numerical integration of the KS equation is the attempt to match the experimental results with those obtained by simulation, in order to be able to design processes that generate surfaces with desired surface topography. Different substrates and conditions were simulated and compared with the experimental work. Figs. 1 and 2 present examples of nanostructured surfaces, with roughened and with patterned topography, respectively.

As our main interest is focused on the patterned topography, we will describe in more detail these simulations and subsequently we will use the results obtained from simulations performed for Si(1 0 0) irradiated with low energy Ar^+ ions as numerical data.

The input parameters were as follows: the angle of the ion-beam incidence was 15° with respect to the normal, the ion flux was $1.8 \times 10^{15}\ cm^{-2}\ s^{-1}$, and the ion energy was 2000 eV. The microscopic quantities were obtained by simulation of the ion implantation by the software package TRIM [10] as follows: the ion range was 2.5 nm, the lateral straggling was 2 nm and the longitudinal straggling was 1.6 nm.

Self-organised ripple patterns evolve on the surface, as presented in Fig. 2. In order to characterize the temporal and spatial evolution of the surface, the height–height correlation function and the interface width defined as the rms fluctuations in the height were used.

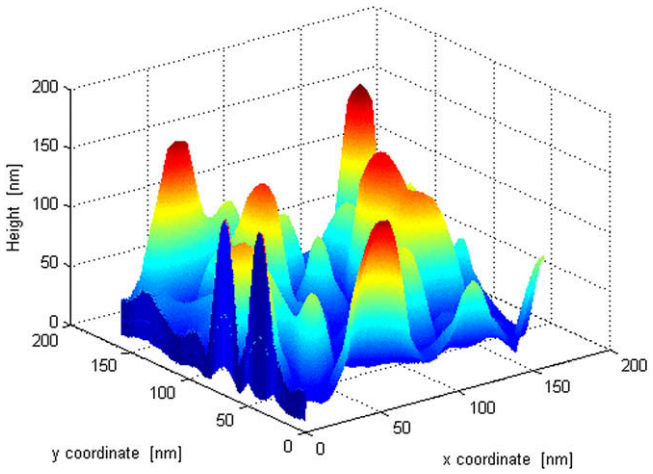

Fig. 1. Example of nanostructured surface: roughened topography. Simulation of Ar^+ ion-beam irradiated Si surface (ion energy $E_{ion} = 2500$ eV, incidence angle $\theta = 75°$, ion flux = $1.8 \times 10^{15}\ cm^{-2}\ s^{-1}$, time = 1000 s).

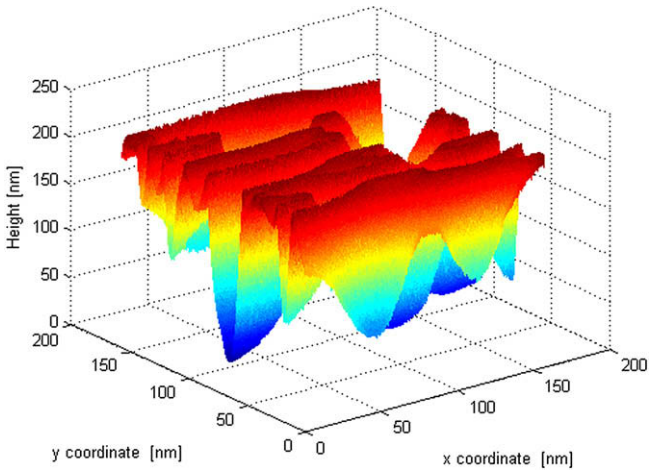

Fig. 2. Example of nanostructured surface: Ripple pattern on Ar^+ ion-beam irradiated Si surface (ion energy $E_{ion} = 2000$ eV, incidence angle $\theta = 15°$, ion flux = $1.8 \times 10^{15}\ cm^{-2}\ s^{-1}$, time = 1600 s).

One important prediction of the simulation, the wavelength of the ripples, is obtained from the height–height correlation function, i.e.,

$$F(r) = \sum_k S(k)e^{-ikr}$$

where $S(k) = \langle h(-k)\, h(k)\rangle$ is the structure factor, calculated from the Fourier transform $h(k)$ of the position of the surface. The position of the peaks in Fig. 3, located clearly visible at approximately 17 nm and approximately 34 nm, allow for the estimation of the ripple wavelength, at approximately 17 nm. For the same conditions, it has been reported [7] that the wavelength measured experimentally is 21 nm. Considering that the theoretical value is approximately 7 nm, we can consider our prediction remarkably precise. Furthermore, the ripple orientation is correctly predicted, along the y axis, as shown in Fig. 2.

The morphology and dynamics of a rough surface can be quantified by the rms height fluctuations:

$$w(L,t) \equiv \sqrt{\frac{1}{L^2}\sum_{x,y=1,L}\left[h(x,y,t) - \overline{h(x,y,t)}\right]^2}$$

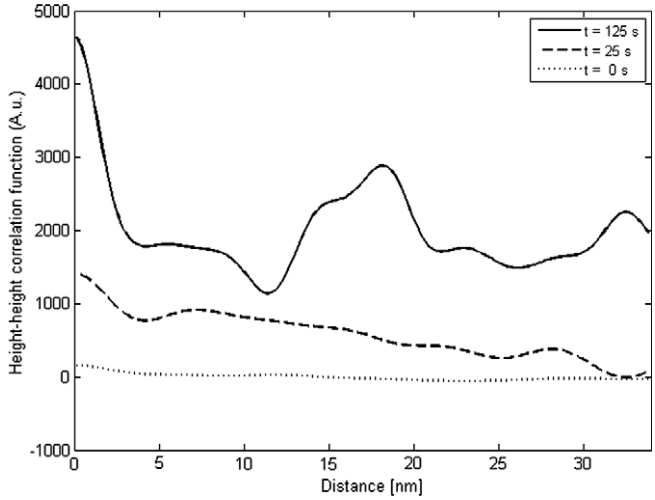

Fig. 3. The height–height correlation function, along the pertinent direction (the other direction is averaged out) for different irradiation times (ion energy E_{ion} = 2000 eV, incidence angle θ = 15°, ion flux = 1.8 × 10^{15} cm^{-2} s^{-1}).

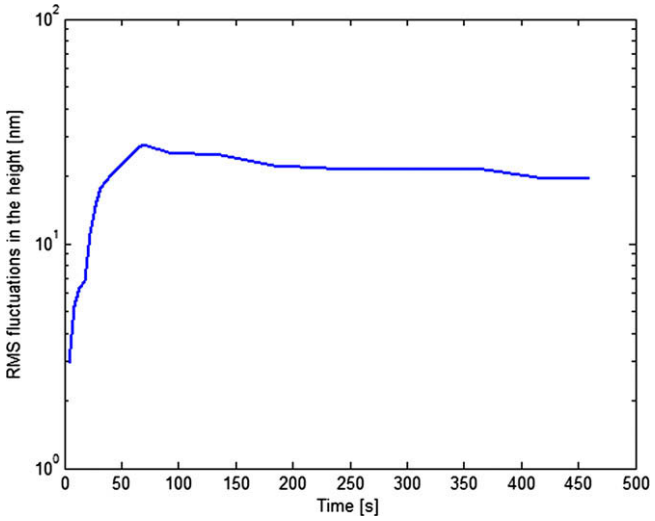

Fig. 4. RMS height fluctuations versus time. For small times, the fluctuations increase exponentially, until the crossover time is reached; for times greater than the crossover time the amplitude of the fluctuations saturates (ion energy E_{ion} = 2000 eV, incidence angle θ = 15°, ion flux = 1.8 × 10^{15} cm^{-2} s^{-1}).

where L is the linear size of the sample and $h(x, y, t)$ is the mean surface height of the surface.

Another prediction of the simulation is the temporal behaviour of the surface topography. For short ion-beam bombardment times, the amplitude of the ripples grows exponentially, then, at a certain time (crossover time), the nonlinear term in KS equation becomes comparable with the linear term, which dictates the exponential growth, and therefore the growth saturates. This behaviour is presented in Fig 4, the evolution of the rms height fluctuations in time.

As alluded before, there are several sources of imprecision of the input variables, which influence the accuracy of the simulations. First, the imprecision regarding the microscopic parameters of the sputter-related quantities (ion range, lateral and longitudinal straggling) can lead to discrepancies in the values of the inputs that can be higher than 400%. This imprecision influences the time evolution of surface morphology and the crossover time, which can lead to early pinching off the ripples and to chaotic behaviour [4]. We think this is the explanation for the fact that the times of bombardment needed to observe the ripples are several times smaller in our simulations than in the experimental work.

With all these qualifications, the simulation qualitatively matches the experimental data, in particular the temporal evolution of the surface nanostructuring. This prediction is even more remarkable keeping in mind that the simulation used several theoretical models for the relationships between the microscopic parameters and the model parameters, importantly influenced by the imprecision in their theoretical values.

4. Conclusions

Ion-beam-induced self-assembly of thin films occupy a special place in the panoply of new nanofabrication technologies, as it combines both the top-down, focused micro-fabrication with the bottom-up self-assembly nano-processes. Our work demonstrates that experimental results can be replicated by simulations, even if the ion-beam-induced self-assembly processes are very sensitive to minute variations of the technological parameters. Furthermore, this study demonstrates that simulation can be used in a feed-forward, design-orientated manner when attempting the fabrication of self-assembled nanostructures with micro-level ion-beam techniques.

Acknowledgments

The reported work has been part of the European FP6 Charged Particle Nanotechnology (CHARPAN) and the FP7 Bio-Inspired Self-assembled Nano-Enabled Surfaces (BISNES) projects.

References

[1] V.A. Shchukin, D. Bimberg, Rev. Mod. Phys. 71 (1999) 1125.
[2] P. Sigmund, Phys. Rev. 184 (1969) 383.
[3] R. Bradley, J. Harper, J. Vac. Sci. Technol. A 6 (1988) 2390.
[4] E. Yewande, A.K. Hartmann, R. Kree, Phys. Rev. B 71 (2005) 195495.
[5] T. Bobek, S. Facsko, H. Kurz, Phys. Rev. B 68 (2003) 085324.
[6] M.A. Makeev et al., Nucl. Instrum. Meth. Phys. Res. B 197 (2002) 185–227.
[7] A. Brown, J. Erlebacher, Phys. Rev. B 72 (2005) 075350.
[8] B. Ziberi et al., Phys. Rev. B 72 (2005) 235310.
[9] M. Castro et al., Phys. Rev. Lett. 94 (2005) 016102.
[10] J. Ziegler, J. Biersack, U. Littmark, The Stopping and Range of Ions in Solids, Pergamon, New York, 1985.